

## Analysis and Evaluation for Trajectories of Paramecia

Shuntaro SHINOHARA<sup>1</sup>, Toshihiro AKIYAMA<sup>1</sup>, Shingo ISHIWATA<sup>2</sup> and Osamu HIRAYAMA<sup>1\*</sup>

<sup>1</sup>Graduate School, Institute of Symbiotic Science and Technology, Tokyo University of Agriculture and Technology, Koganei-shi, Tokyo 184-8588, Japan

<sup>2</sup>Department of Physics, Faculty of Engineering, Yokohama National University, Yokohama-shi, Kanagawa 240-8501, Japan

\*E-mail address: hrym@cc.tuat.ac.jp

(Received February 25, 2005; Accepted December 7, 2005)

**Keywords:** Paramecium, Trajectory, Localized Direction Change (LDC), Random Walk, Evaluation Function

**Abstract.** Trajectories of paramecium observed with a microscope were analyzed and it was found that they are composed of four components, namely, Segment, Wavelike form, Arc and Localized Direction Change (LDC). Similar experiments were conducted also in the case that temperature gradient exists and the frequencies of LDC per unit time were measured in both cases. Angle distributions in direction changes and some fitting functions were obtained. It was clarified that the frequency of LDC in the case that the paramecium moves toward the proper temperature area is less than toward improper one. It was confirmed that random walk time scales were nearly equal to the average time interval of LDC. Numerical simulations were conducted and the optimum value for the probability of LDC per unit time which maximize the evaluation function was obtained.

### 1. Introduction

The movement of a paramecium is nearly random walk motion. Namely, paramecia proceed straight ahead almost time, and they then change the directions of movements suddenly by random angles and natures of this random walk motion have been investigated in detail (HARA, 1984; SATO and FUJIMURA, 1992). On the other hand, there exists a report that the representative moving trajectory of paramecia in a three dimensional space is a spiral (SUGINO and NAITOH, 1988). It is supposed that the difference between above-mentioned two arguments originates from the difference between observation time scales of each standpoint. In order to clarify this point, trajectories of paramecia were observed, and the components of the trajectories were examined in the case that movements of paramecia were reduced to two-dimensional ones. Analyses for the trajectories were conducted from some points of view; angle distributions in the direction changes, average time intervals of the localized direction change, and the relationship between the average displacement and corresponding time.

The fact is also known that paramecia remember their cultivated temperature as the

proper one and frequencies of the direction change tend to be different from each other in the case they move towards the proper temperature and towards the improper (NAKAOKA and OSAWA, 1977; NAKAOKA and TOYOTAMA, 1980; HARA, 1984).

As for the mechanism for direction change the following facts have been already known. When the electric potential in a paramecium body exceeds a critical value, it changes moving directions by vibrating its cilia (OSAWA, 2001). A change of electric potential is realized by opening and closing potassium and calcium channels. In the case towards the improper temperature, the electric pulses (or noises) are generated more frequently and the frequency for the electric potential to exceed the critical values becomes larger than toward the proper one. This mechanism is called stochastic resonance. It has been known that some kinds of organisms adopt the principle of stochastic resonance (DOUGLASS *et al.*, 1993; RUSSELL *et al.*, 1999). Consequently, paramecia continue to move towards the proper temperature in total, and simultaneously they do not stay at one position of the proper temperature. This tendency brings a merit which makes paramecia to explore multiple locations of the proper temperature in a wide range, since if they reach to a location of the proper temperature they have chances to escape from this location and visit to other locations of the proper temperature. Some numerical simulations were conducted in order to confirm this standpoint. In the simulations, we propose an evaluation function by which the advantage of the characteristic of paramecia is quantified and investigate the probabilities of the localized direction change which maximize the evaluation function.

The purpose of this thesis is to report the results of these problems.

## 2. Method of Observation

### 2.1. Observation

In order to take video pictures of trajectories of paramecia, the apparatus shown in Fig. 1 was set up. A water drop containing some paramecia is located on an aluminum plate and covered with a cover glass. The depth of the water drop is limited about 0.1 mm by covering with the cover glass, which reduces movements of paramecia to two-dimensional ones actually. Tele-video scope was set up above the cover glass and motions of paramecia in the sight (10 mm × 10 mm) were recorded in a video film through the video scope. The lights were projected from one side and the bottom of the aluminum plate was painted with black paint in order to make the contrast clear. In the case that a temperature gradient was set up, Peltier module were placed on the both side of the aluminum plate.

In order to clarify the influences of temperature and its gradient to movements of paramecia, observations of moving trajectories of paramecia in the following six temperature environments, and their data analyses were conducted. Different group of *Paramecium caudatum* were used in each case (hereafter called as "Paramecium"), however all groups were cultivated in 25°C temperature, which means the proper temperature is set up as 25°C in the present research. The genetic origin of paramecia used in the observation is unknown, which was not paid much attention to since the present research is based on the different standpoint from the biological one.

Case-1. 10 trajectories in 20°C (without temperature gradient)

Case-2. 10 trajectories in 25°C (without temperature gradient)

Case-3. 10 trajectories in 28°C (without temperature gradient)

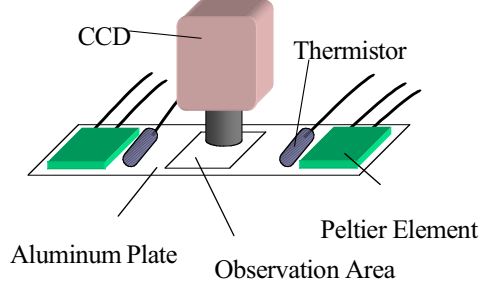


Fig. 1. Schematic of apparatus for observation.

Case-4. 11 trajectories in 25°C–20°C (with temperature gradient)

Case-5. 12 trajectories in 25°C–28°C (with temperature gradient)

Case-6. 10 trajectories in 27°C–20°C (with temperature gradient)

Each trajectory of paramecia is constructed with its pictures at every 0.1 sec.

## 2.2. Analysis

The angle of direction change  $\theta$  was calculated from the coordinates of the points just before and after the change of direction as follows.

First, the displacement vector between  $(n-1)$ -th time step and  $n$ -th time step is obtained as  $\mathbf{D}_n = (x_n - x_{n-1}, y_n - y_{n-1})$  from the coordinates at both time steps. Then the angle between vector  $\mathbf{D}_n$  and y-axis is obtained as

$$\theta_n = \arctan\left(\frac{x_n - x_{n-1}}{y_n - y_{n-1}}\right)$$

in the case that

$$D_n = \sqrt{(x_n - x_{n-1})^2 + (y_n - y_{n-1})^2} > D_c,$$

where  $D_c$  is a critical value mentioned just later. Next,  $\theta_{n+1}$ , the angle between the displacement vector at the next time interval and y-axis is calculated in the same way and the angle of direction change  $\theta$  is given as

$$\theta = \theta_{n+1} - \theta_n.$$

In the case of  $D_n < D_c$  it is difficult to determine these angles with sufficient accuracy. It is regarded that a paramecium changes its moving direction after some time units stay in the small circle area in this case (we estimated its diameter  $D_c$  as 0.25 mm, the average body length of a paramecium). We call this case as localized direction change (LDC). The cases

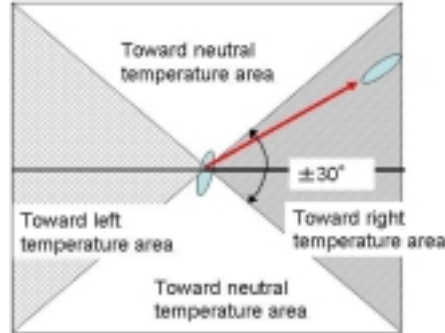


Fig. 2. Definition of the proper temperature-, improper temperature- and neutral-direction.

other than LDC should be called as continuous direction change. LDC corresponds to the case in which the linear motion of a paramecium can be neglected. The angle of direction change  $\theta$  in LDC is defined as the angle between the straight segment incident on this small area and that emitted from this area. This definition for the angle of direction change is similar to that given in some previous research for in vitro motility of F-actin fragments (SHIKATA *et al.*, 1994). We should notice that no thresholds were set up for the angle of direction change in LDC and nearly null angle cases were contained in LDC.

The angle distributions for all direction change containing LDC in the cases without temperature gradient and those in the cases with temperature gradient were examined. The average value  $\mu$  and standard deviation  $\sigma$  of angle of direction change were calculated for these cases. The skewness and the kurtosis defined as

$$\text{Skewness} = \frac{\langle (\theta - \mu)^3 \rangle}{\sigma^3}, \quad \text{kurtosis} = \frac{\langle (\theta - \mu)^4 \rangle}{\sigma^4},$$

were also calculated for these cases where square brackets indicate that the average values of the quantities in the bracket are taken.

We paid much attention to LDC, since we think that a random walk motion of a paramecium is caused by LDC. Then, time intervals of every LDC were counted for all trajectories in all cases and the time interval distributions of LDC were investigated.

In the case that a temperature gradient was set up we classify LDC into the following nine types, namely, one from the proper temperature region to the proper, one from proper to neutral, one from proper to improper, one from neutral to proper, one from neutral to neutral, one from neutral to improper, one from improper to proper, one from improper to neutral and one from improper to improper, where the direction to the proper temperature is designated as a region held between the line inclined at  $-30^\circ$  to the perpendicular line to the proper temperature boundary and that at  $+30^\circ$ , and so on (shown in Fig. 2).

Next, we search for the time unit on which a trajectory of a paramecium can be regarded as a random walk. In the case of a classical random walk the average value of

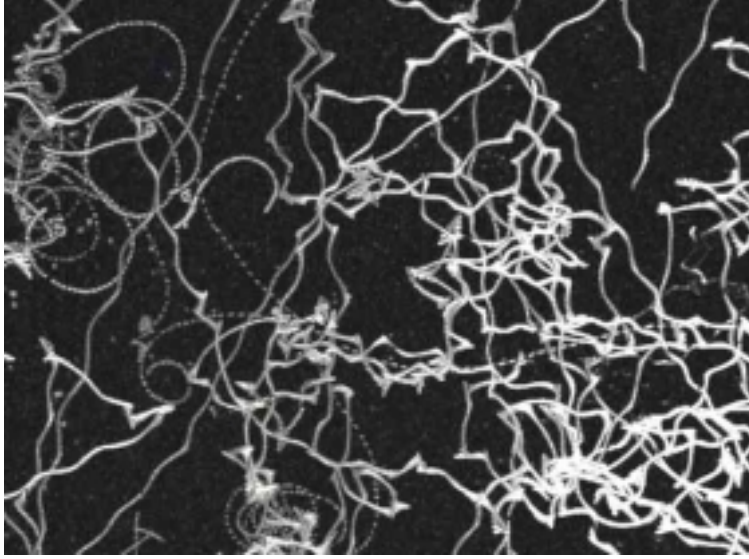


Fig. 3. An example of video picture for trajectories of paramecia

square of the distance from the starting point  $\langle r^2 \rangle$  is proportional to the corresponding time  $t$ , while in the case of a straight forward movement  $\langle r^2 \rangle$  is proportional to  $t$ . Here, the value  $\langle r^2 \rangle$  corresponding to the time interval  $t = m\Delta t$  for each trajectory is calculated as follows:

$$\langle r^2 \rangle_m = \frac{\sum_{i=1}^{N-m} \left[ (x_{i+m} - x_i)^2 + (y_{i+m} - y_i)^2 \right]}{N - m},$$

where  $\Delta t$  is the time unit, on which the moving distances are measured,  $m$  an integer and  $N$  the total number of time steps in each trajectory. Here, we compare the relationships between  $\langle r^2 \rangle$  and  $t$  in cases of  $\Delta t = 2$  s (almost average time interval of LDC) with that in case of  $\Delta t = 0.1$  s (minimum time unit in observation). In the former case the coordinates of a paramecium at every 2 seconds are extracted from the original data and the values of  $\langle r^2 \rangle$  is calculated according to the above definition (actually the range of  $m$  is restricted so that  $m < N/2$  in order to avoid few sample number cases).

### 3. Results

#### 3.1. Classification of the components of trajectories

An example of the video pictures is shown in Fig. 3. Nine examples of the trajectories in the case without temperature gradient (Case-1, -2, -3) and nine with temperature gradient (Case-4, -5, -6) were shown in Figs. 4 and 5 respectively. In these figures the dots designate

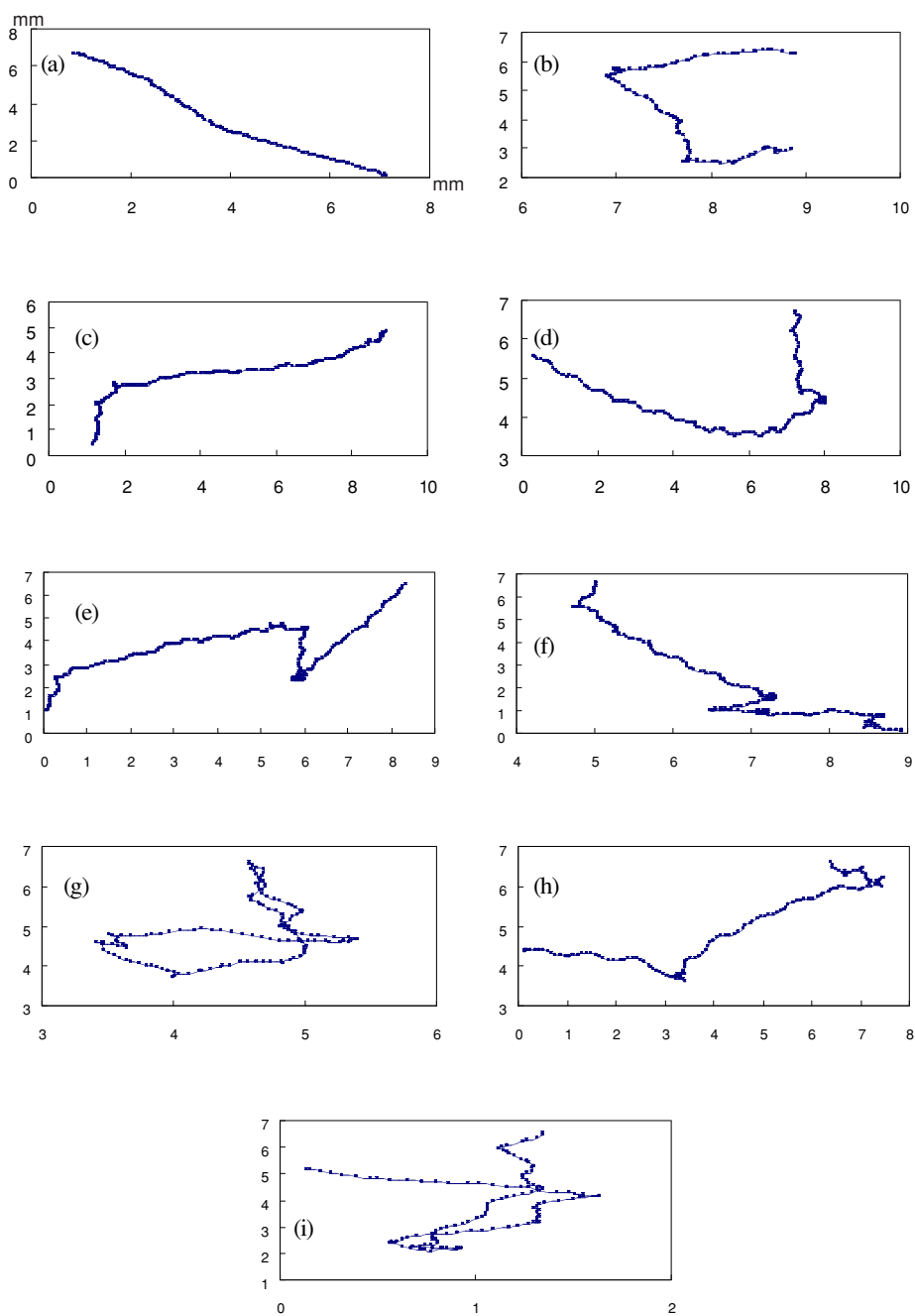


Fig. 4. Examples of trajectories of paramecia. (a)–(c) in the case of 20°C (without temperature gradient), (d)–(f) in the case of 25°C, and (g)–(i) in the case of 28°C. Components of trajectories are shown in Table 1.

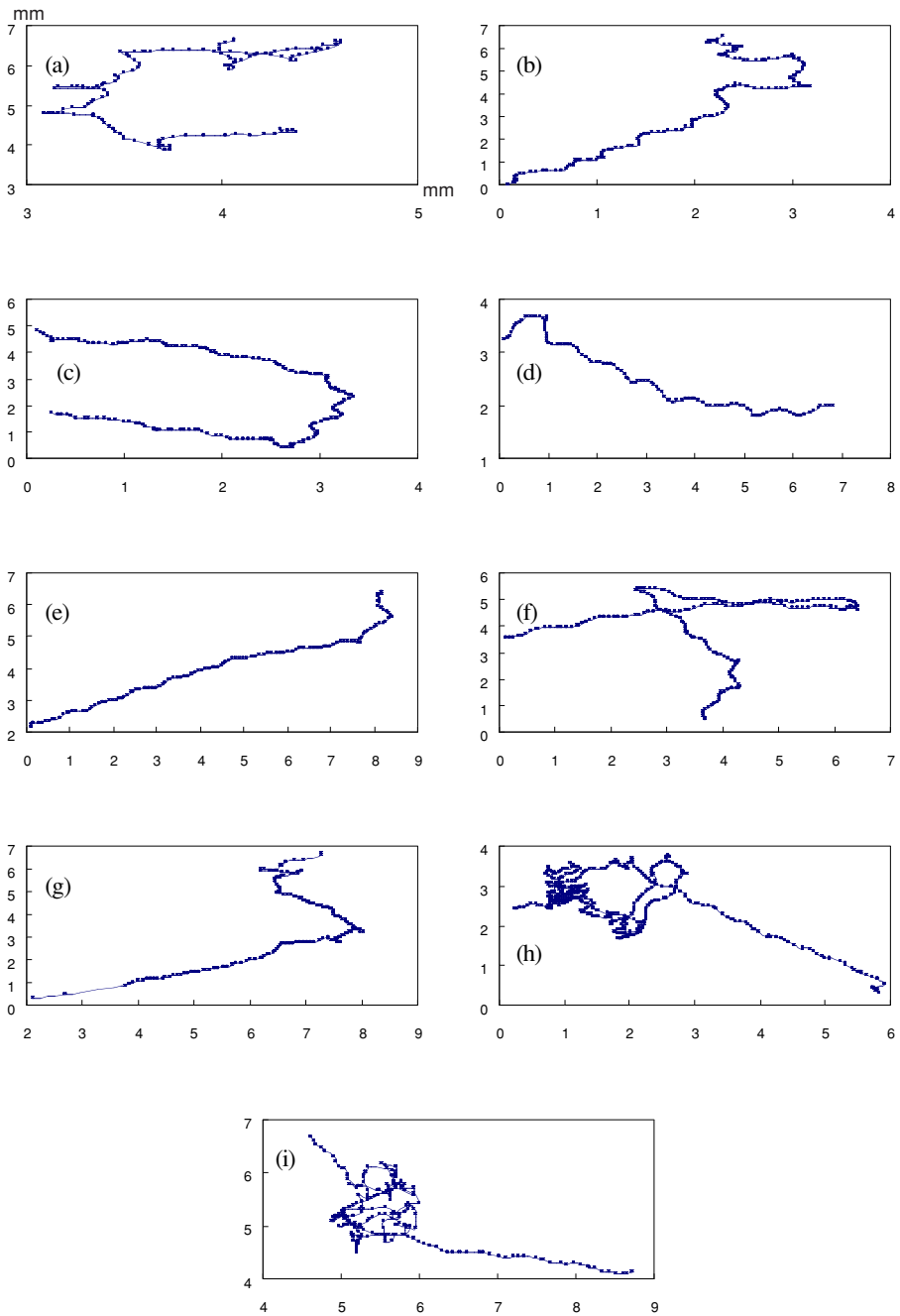


Fig. 5. Examples of trajectories of paramecia. (a)–(c) in the case of  $25^{\circ}\text{C}$ – $20^{\circ}\text{C}$  (with temperature gradient), (d)–(f) in the case of  $25^{\circ}\text{C}$ – $28^{\circ}\text{C}$ , and (g)–(i) in the case of  $27^{\circ}\text{C}$ – $20^{\circ}\text{C}$ . Components of trajectories are shown in Table 1.

Table 1. List of the examined trajectories.

Case number	Components of trajectory	Corresponding figure number
Case-1 (20°C)	Segment	Fig. 4(a)
	Segment + LDC	Fig. 4(b)
	Segment + LDC	Fig. 4(c)
Case-2 (25°C)	Wavelike + LDC	Fig. 4(d)
	Segment + Wavelike + LDC	Fig. 4(e), Fig. 8(c)
	Segment + Wavelike + LDC	Fig. 4(f)
Case-3 (28°C)	Segment + Arc + LDC	Fig. 4(g)
	Wavelike + LDC	Fig. 4(h)
	Segment + Arc + LDC	Fig. 4(i)
Case-4 (25°C–20°C)	Segment + LDC	Fig. 5 (a), Fig. 8(a)
	Segment + Wavelike + LDC	Fig. 5 (b)
	Segment + Wavelike + LDC	Fig. 5 (c)
Case-5 (25°C–28°C)	Wavelike + Arc + LDC	Fig. 5 (d), Fig. 8(b)
	Segment + Wavelike + LDC	Fig. 5 (e)
	Segment + Wavelike + LDC	Fig. 5 (f)
Case-6 (27°C–20°C)	Segment + LDC	Fig. 5 (g)
	Segment + Wavelike + Arc + LDC	Fig. 5 (h)
	Segment + Wavelike + LDC	Fig. 5 (i)

the locations of the center of a paramecium at every 0.1 second. From these figures we can find that the trajectories are consisted of four kinds of factors approximately as follows:

- (1) Segment which is almost straight (hereafter called as Segment);
- (2) Wavelike form (hereafter called as Wavelike);
- (3) Arc (almost whole circle or semi-circle);
- (4) Localized direction change (“LDC”).

Although it is difficult to give these factors exact definitions, it is available to classify each part of the trajectories into these factors since it makes our pattern recognitions for trajectories of paramecia possible with ease. The form of each trajectory can be approximately explained with these terms. For example, the case 1 (shown in Fig. 4(a)) is consisted of the some “Segment” s, the case 3 (shown in Fig. 4(d)) some “Segment” s and “LDC” s and so on. The components of each trajectory are shown in the Table 1. In the case of LDC paramecium stays at almost one position during an “LDC”

### 3.2. Angle distributions in direction change in all trajectories

The angle distributions for Case-1, -2, -3 (without temperature gradient case) were shown in Fig. 6(a) and those for Case-4, -5, -6 (with temperature gradient) in Fig. 6(b). Average, Standard deviation, Skewness and Kurtosis of the angle distribution in all cases are listed in Table 2. It is known that in the case of Gaussian distribution the value of the

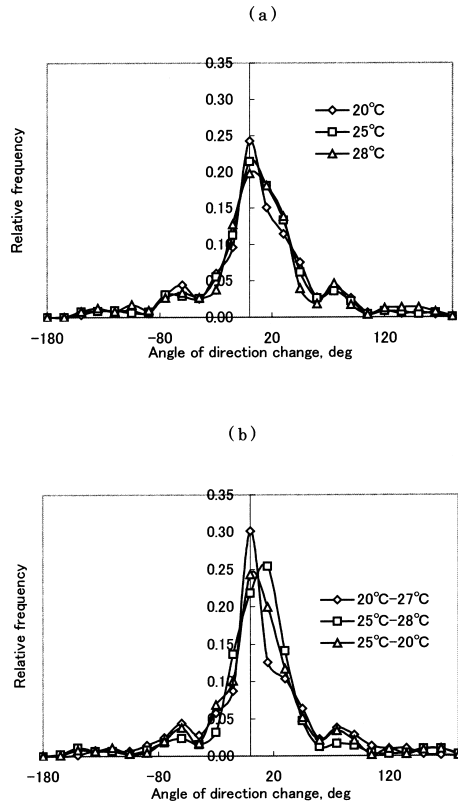


Fig. 6. Angle distributions in all direction change in case (a) without and (b) with temperature gradient.

skewness and the kurtosis are 0 and 3 respectively.

We can find from these figures and table that the distributions are almost symmetric for the vertical axes (the Average are negative for all cases, however the absolute values of them are less than  $0.4^\circ$  in all cases, and the absolute values of Skewness are less than 0.2 in all cases). It should be noted that Standard deviations are within the range  $46\text{--}54^\circ$  in all cases. The value of kurtosis is larger than that of Gaussian, 3.0 in all the cases, which means that the frequencies for extremely small and large angles are larger than those for Gaussian and those for intermediate angles are smaller. It was examined whether these angle distributions are fitted by some analytical functions or not, and it was found that these distributions are well fitted by the function

$$f(\theta) = \frac{\beta}{\left((c\theta)^2 + \alpha^2\right)^{\frac{1+\beta}{2}}}$$

Table 2. List of characteristic values of angle distributions in all direction change and average time interval LDC for each case. The symbols (p), (i), (l), and (r) denote the case in which the paramecia move towards proper, improper, left-side and right-side temperature respectively.

Case number	Characteristics of angle distribution				Total number of LDC	Average time interval of LDC
	Average	Standard deviation	Skewness	Kurtosis		
Case-1 (20°C)	-0.01°	48.1°	-0.14	4.418	188	4.20 sec
Case-2 (25°C)	-0.17	48.2	-0.17	5.014	66	3.79 sec
Case-3 (28°C)	-0.03	53.8	0.060	4.609	119	1.62 sec
Case-4 (25°C–20°C)	-0.12	47.4	0.020	5.644	100	3.31 s (p), 1.89 s (i)
Case-5 (25°C–28°C)	-0.34	46.3	-0.12	7.104	53	3.04 s (p), 2.21 s (i)
Case-6 (27°C–20°C)	-0.09	47.0	0.030	4.255	246	1.73 s (l), 1.19 s (r)

as shown in Fig. 7, where  $\theta$  is angle of direction change. The fitting curves of this type were introduced by the reason that these distribution functions could be related to Cauchy distribution (Lorenz distribution) for some parameter values (TAKAYASU, 1986). Actually, by introducing the normalized angle  $\eta = c\theta/\alpha$ , this distribution function are rewritten as

$$F(\eta) = \frac{b}{(1 + \eta^2)^{\frac{1+\beta}{2}}}$$

where  $b$  is constant and in case that  $\beta = 1$ , this distribution function reduces to Cauchy distribution. The value of  $\beta$  is 0.242 (in case (a)) and 0.926 (in case (b)) respectively, and in the latter case this distribution function can be regarded as Cauchy distribution approximately. Furthermore, the asymptotic behavior of above function is  $F(\eta) \approx \eta^{-(1+\beta)}$  at  $|\eta| \gg 1$ , which coincide with that of Levy-distribution (OTA, 2000). Though the behavior of the angle distribution is similar to those of Levy distribution in the asymptotic range, it was clarified the behavior of these distributions are hardly regarded as Levy distribution at small  $\theta$  range.

The angle distributions for LDC are shown in Fig. 8. We can see from these figures that these angle distribution is not perfectly flat, which suggests that even in case a paramecium change its direction after some time units stay in a small circle area, the larger the rotation angle is the smaller its frequency becomes.

### 3.3. Time interval of LDC

Time interval distribution in Case-2 (25°C, without temperature gradient) and in Case-4 (25°C–20°C) are shown in Fig. 9. The average value of time interval of LDC is 3.79 sec in Case-2, where the temperature environment is proper and without temperature gradient. In the case with temperature gradient the distribution is shifted to the smaller part in total than in Case-2. We can also find that this tendency is remarkable in case that paramecia

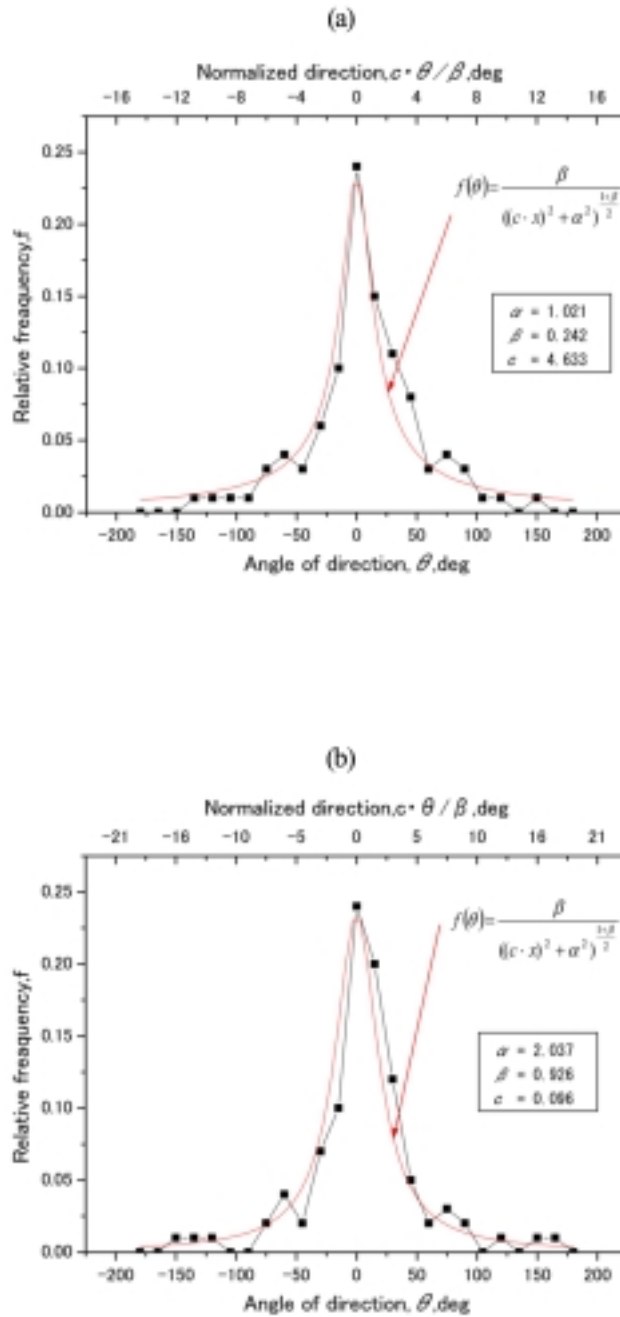


Fig. 7. Angle distributions in all direction change and their fitting curves in case (a) without temperature gradient (25°C) and (b) with temperature gradient (25°C–20°C). The horizontal scales at the top of the graphs denote the normalized angle  $\eta = c\theta/\alpha$ . The parameter values are shown in the figures.

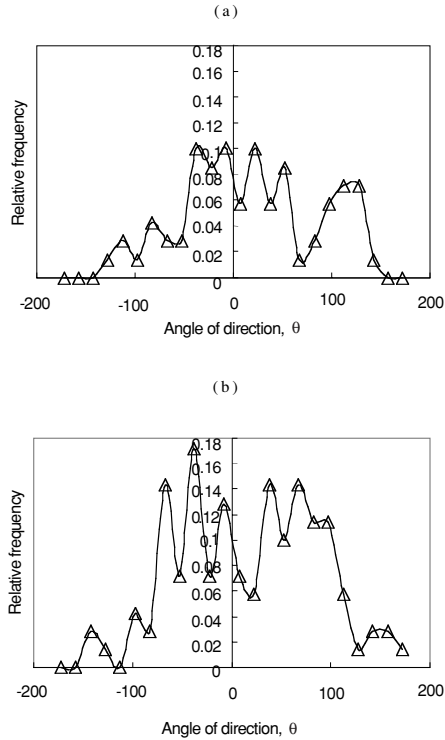


Fig. 8. Angle distribution in LLADC in the observations in case of (a) without temperature gradient (25°C) and (b) with temperature gradient (25°C–20°C).

move toward the improper temperature (20°C) than toward the proper one (25°C). The average values of each case are 1.89 sec and 3.31 sec, respectively.

The total number of LDC and the values of average time intervals for all cases are listed in Table 2. The tendency that paramecia causes LDC more frequently in case they move towards the improper temperature than towards the proper one was observed clearly in Case-4 and Case-5. In Case 6, the average time interval of LDC in case towards 27°C is pretty larger than towards 20°C. It might be explained from the fact that 27°C is closer to the proper temperature (25°C) than 20°C.

### 3.4. Confirmation of the time scale for random walk

Some examples of relationships between the average value of square of the distance from the starting point  $\langle r^2 \rangle$  and the corresponding time  $t$  with and without temperature gradient cases are shown in Fig. 10. We can see from these figures that  $\langle r^2 \rangle$  is almost proportional to time  $t$  in case of  $\Delta t = 2$  s, which suggests that the moving trajectories of paramecium can be regarded as random walk motions if we adopt the average time interval of LDC as time unit. No these results in case of  $\Delta t = 0.1$  s show that  $\langle r^2 \rangle$  is proportional

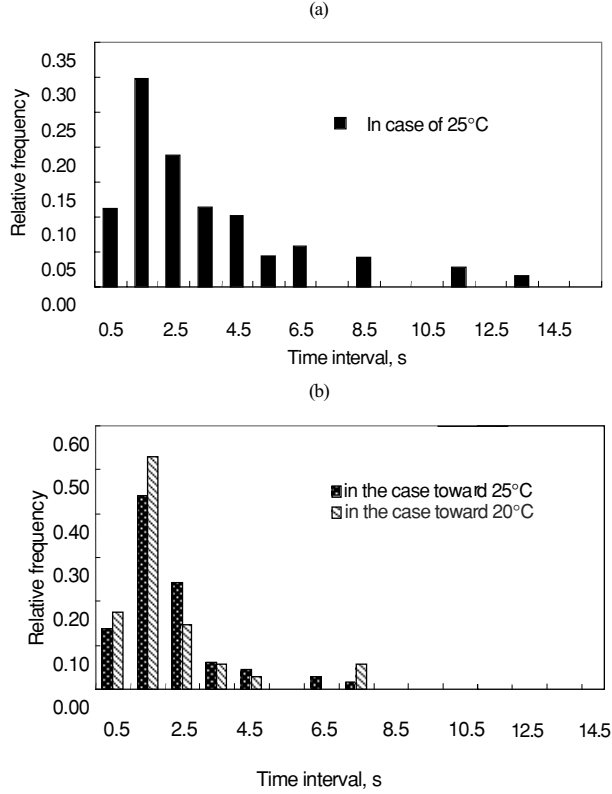


Fig. 9. Average time interval distributions in LLADC in case (a) without and (b) with temperature gradient.

to time  $t$ , which suggests that the moving trajectories of the paramecia can be regarded as almost straight line in the short time scales.

## 4. Simulations

### 4.1. Method of numerical simulations

A numerical simulation based on above-mentioned data was conducted. The following algorithm was adopted.

First, an area is a square which consisted of  $600 \times 600$  grids. Nine higher temperature points with  $30^\circ\text{C}$  are located with same intervals in the area and minimum temperature points with  $10^\circ\text{C}$  are located on the center of the four neighboring proper temperature points. The temperature distribution function  $T(x, y)$  was set up as

$$T(x, y) = 10 + 5 \left[ \sin\left(\frac{2\pi x}{200} - 1\right) + \sin\left(\frac{2\pi y}{200} - 1\right) + 2 \right],$$

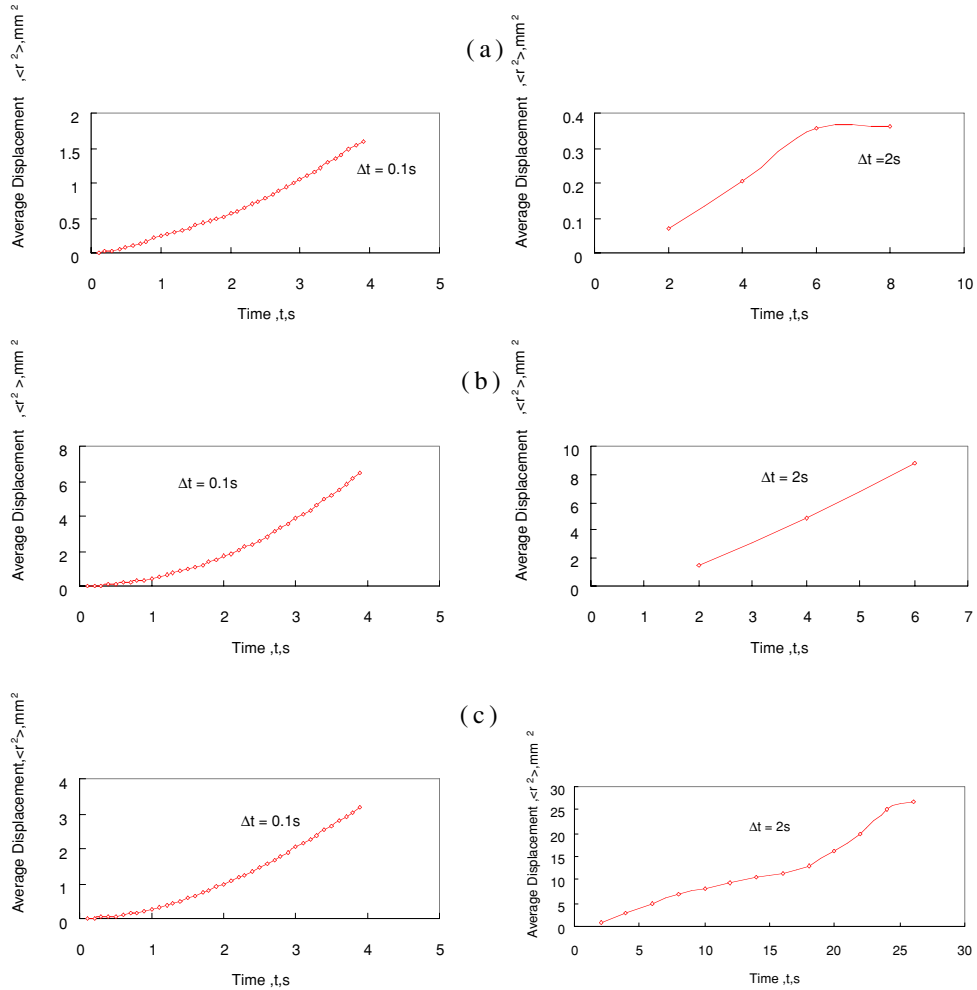


Fig. 10. Examples of the relationship between  $\langle r^2 \rangle$  and  $t$  in the case that  $\Delta t = 2$  sec and 0.2 sec for the case of (a) 25°C–28°C, (b) 25°C–20°C and (c) 25°C.

and the areas with the temperature range between 26°C–24°C were assumed as proper temperature areas ( shown in Fig. 11(a)).

In giving the governing rule for the movements of a paramecium we assume that they are consisted of two categories, straightaway motion and direction change with random angle distributions correspond to LDC in observation. The moving distance in one step is set up as 5 grids. Distance between two points separated by 5 grids is regarded 1.0 mm, since the average velocity of paramecium is about 1 mm/s and the time unit in the simulations corresponds to 1 sec. It is assumed that a paramecium can detect the temperature at present location and compare it with that at the location one time step before, and change



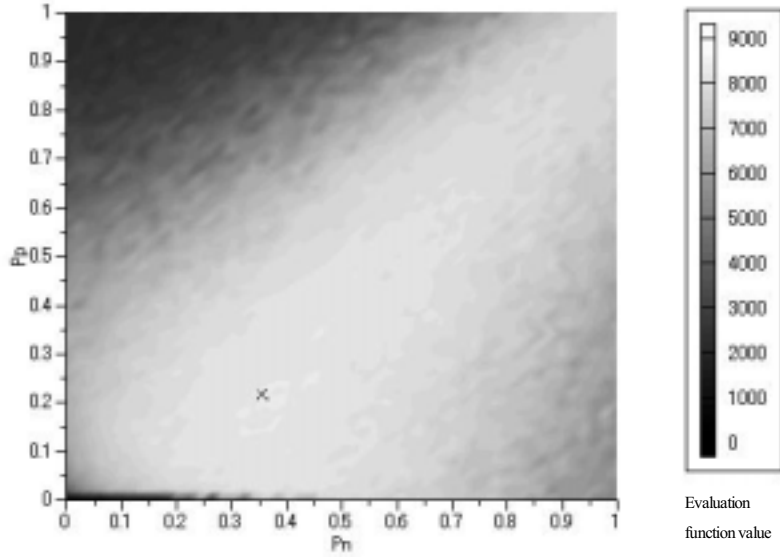


Fig. 12. Distribution of the values of evaluation function for each combination of  $P_p$  and  $P_n$ .

$$F = \sum_{x,y} f_T(x,y)f_N(x,y), \quad f_T(x,y) = \exp[-\gamma \cdot |25 - T(x,y)|],$$

$$f_N = \sum_{n=1}^N \exp[-\delta(n-1)] = \frac{1 - \exp(-\delta N)}{1 - \exp(-\delta)},$$

where  $T(x, y)$  denotes the temperature at location  $(x, y)$  and  $N$  the frequency of visit to location  $(x, y)$ . This evaluation function is originally proposed in the present research. The first factor  $f_T$  expresses the effect that the nearer to 25 °C the temperature is, the larger the value accompanied with the point is. The factor  $f_N$  expresses the effect that the larger the frequency of the visit to a same location becomes, the smaller the values newly added to  $F$  is.

Computations for several values of  $P_p$  and  $P_n$  were conducted and the combination of  $P_p$  and  $P_n$  which maximizes  $F$  was searched for under some values of  $\gamma$  and  $\delta$ .

#### 4.2. Results of numerical simulations

Results under the condition that  $\gamma = 0.007$ ,  $\delta = 2.0$  are shown in Figs. 11(b)–(d). In the case that  $P_n = 1.0$  and  $P_p = 0$ , while factor  $f_N$  is large, the number of the visited proper temperature area is only two (shown in Fig. 11(b)), which brought the low value of  $F$ . In the case of  $P_n = 0.03$ ,  $P_p = 0.03$ , in contrast, while the number of visited proper area is large, the value of  $f_T$  becomes very small (shown in Fig. 11(c)), which also brought low value of

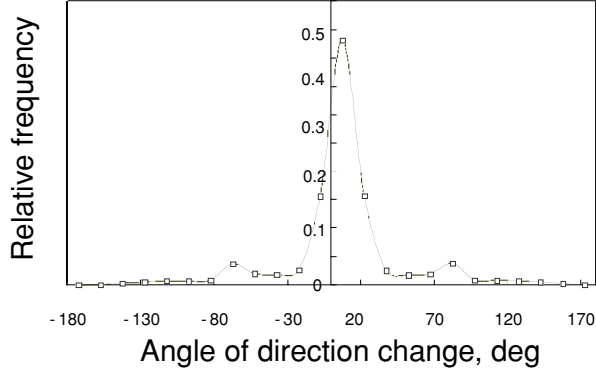


Fig. 13. Angle distribution of direction change in the simulation.

$F$ . In the case of  $P_n = 0.36$ ,  $P_p = 0.22$  ( $P_n/P_p = 1.6$ ), the maximum value of  $F$  was obtained (shown in Fig. 11(d)). The distribution of evaluation function  $F$  for all combination of  $P_p$  and  $P_n$  is shown in Fig. 12.

In the case that  $\gamma = 0.007$ ,  $\delta = 2.0$ , the ratio of  $P_n$  to  $P_p$  which maximizes  $F$  is obtained as  $P_n/P_p = 0.36/0.22 = 1.6$ . On the other hand, the value of  $P_n/P_p$  in observation is obtained, for example, as  $0.53/0.30 = 1.77$  in Case-4 in Table 2 (the value of  $P_n$ ,  $P_p$  in observation are obtained as the inverse of average time interval of LDC 1.89 s and 3.31 s). Both values almost coincide with each other. The angle distribution of the all direction change in this case is shown in Fig. 13. The comparison between the angle distribution in Fig. 13 and those in Fig. 7(b) is given in the next section.

## 5. Discussions

Here, we mention some comments about the angle distribution for direction change.

First, we mention about the accuracy of the determination of angle  $\theta$ . It is supposed that  $\Delta\theta$ , the error in  $\theta$  is mainly caused by the error generated in the process of reading  $x$  and  $y$  coordinates. If the angle  $\theta$  is determined by the expression  $\theta = \arctan(\Delta x/\Delta y)$  and the infinitesimal errors  $\xi$  and  $\zeta$  are introduced to the reading value of  $\Delta x$  and  $\Delta y$  respectively, the error  $\Delta\theta$  can be estimated as

$$\Delta\theta = \frac{\partial\theta}{\partial(\Delta x)} \xi + \frac{\partial\theta}{\partial(\Delta y)} \eta = \frac{\Delta y \cdot \xi + \Delta x \cdot \zeta}{(\Delta x)^2 + (\Delta y)^2}.$$

If  $\Delta x$  and  $\Delta y$  are assumed to be same order, the order of  $\Delta\theta$  is regarded as

$$O(\Delta\theta) = O(\xi / \Delta x).$$

The magnitude of  $\xi$  is estimated as 0.014 mm which corresponds to 1 pixel. The minimum value of  $\Delta x$ , which gives the maximum value of  $\Delta\theta$ , can be regarded as the diameter used for the definition for LDC, and is given as about 0.25 mm, the twice of the paramecium body length. Thus, the maximum value of  $\Delta\theta$  is given as  $\Delta\theta = 0.014/0.25 = 0.056 \text{ rad} = 3.2^\circ$ . This value is much smaller than that of angle interval in the angle distributions in Fig. 7.

Secondly, we mention about the comparison between the angle distributions shown in Fig. 7(b) (the case with temperature gradient  $20^\circ\text{C}$ – $25^\circ\text{C}$  in the observation) and in Fig. 13 (the case of  $P_n = 0.36$ ,  $P_p = 0.22$  in the simulation). At a first look both distributions seem to be similar to each other, however, by more precise observation we can find that the latter has a sharper peak around the null direction change than the former. The reason of this difference can be explained as follows. In the case of Fig. 7(b) the probability of LDC per unit time  $P_p$  and  $P_n$  are given as  $P_n = 0.53$ ,  $P_p = 0.30$ , which is pretty larger than those in Fig. 13. Furthermore, the angle distribution in Fig. 7(b) contains both the events originated from angle change for LDC and those for others (continuous direction change), while in Fig. 13 only from LDC. As a result the rate of null angle change (corresponding to straight forward case) is higher in the case of Fig. 13 than in Fig. 7(b).

As for the comparison between the present research and other ones, some results for the angle distribution in the temporal evolution of the position of the center of the mass in human postural sway is known (TAKADA *et al.*, 2001). They obtained the result in the observation that the frequency in the small direction change is large, while it is flat in the simulation. It is supposed that they used the model that random external forces are applied at every time steps in their simulation (the external forces is given by pseudo random number (LEHRER, 1951)). On the other hand, in the simulation of the present research, one random direction change of a paramecium is given in several time steps and null angle direction change is also included in the total number of direction change, which brings no perfectly flat distributions. As for the angle of direction change for in vitro motility of F-actin fragments (SHIKATA *et al.*, 1994; SHIMO and MIHASHI, 2001), the effect of the length of F-actin was taken into considerations. Especially it was clarified by SHIKATA *et al.* (1994) that the angle distributions of direction change of F-actin depend on its body length. On the other hand, in the present research the length of paramecium is taken into consideration only for the estimation for  $D_c$  and the movement of the center of mass of a paramecium is treated.

Thirdly, we consider the effects of the sampling time on the angle distribution. By assuming that the moving velocity of a paramecium is 1 mm/s, its body length 0.2 mm, we can estimate the time to travel the distance of its body length is about 0.2 s. It is supposed that if we had adopted much shorter sampling time than this value, the errors in the measurement would have been much larger than the present ones. On the other hand, it is supposed that in the case of much larger sampling time (for example,  $\Delta t = 2 \text{ s}$ ) the angle distribution would be too flat, since the trajectories approaches to those for random walks. Then we think that the value of the sampling time used in the present research,  $\Delta t = 0.1 \text{ s}$ , is an appropriate one to examine the angle distributions.

Next, we add some comments for the simulation.

First, we mention about the way of setting up the evaluation function. Two parameters  $\alpha$ ,  $\beta$  are contained in the present evaluation function, and it should be noted that the values of  $P_n$  and  $P_p$  which maximizes  $F$  are different from the present one in case of other sets of

$\gamma$ ,  $\delta$ . Furthermore, other forms than the present ones for  $f_T$  and  $f_N$  would be possible if they had similar behavior to those of present ones. In this sense what we could clarify in the present research is that the values obtained in the observation for probabilities of LDC maximize the evaluation function if an evaluation function and parameter values contained in it are adopted appropriately. Although we have no means to determine the unique form of evaluation function, we think it is important that behaviors of paramecia can be accounted for by the idea that they behave so that an evaluation function is maximized or minimized.

Second, it is assumed in the present simulation that a paramecium can know the temperature gradient by detecting the temperature values at different locations corresponding to successive two time steps. This assumption is based on the fact that the reactions of paramecia to temperature are caused by the temporal derivative of temperature not by the spatial gradient of it directly. The value of the temporal derivative of temperature set up in the present simulations is about 0.5 deg/s if the average speed of paramecium is regarded 1 mm/s, which exceeds the critical value of temporal derivative of temperature which cause the reaction of paramecia, 0.055 deg/s, sufficiently (NAITO, 1990).

Third, we mention about the relationship between the algorithm of the present simulation and stochastic resonance. Although we noticed that the mechanism of stochastic resonance lies beyond the apparent behaviors of paramecia, we did not adopt an algorithm which directly related to stochastic resonance and contains electric potential of paramecium. One reason is that no electric potentials were measured in the present research and we could have given no comparisons between the electric potentials in simulation and those in experiments. Another reason is that we can reach the purpose of the present research through the way of the present simulation, which is based on the apparent behavior of paramecia such that the probability of LDC depend on whether they moves towards the proper temperature or not.

Lastly we mention about the future subjects. It has been pointed out that behaviors of paramecia depend on the number density of them. Standing at this point some correlations and interactions between neighboring trajectories should be examined in the above-mentioned analyses and also numerical simulations for behaviors of plural paramecia should be conducted. We are planning these researches as next subjects.

## 6. Conclusions

The main conclusions of the present research are summarized as follows.

First, the trajectories of paramecia are consisted of four kinds of factors, "Segment", "Wave-like pattern", "Arc" and "LDC" (Localized Direction Change).

Second, the angle change distributions for all trajectories in the cases with and without temperature gradient were obtained, and it was found that the kurtosis of the present distributions were larger than that of Gaussian distribution, and some fitting function were obtained.

Third, it was clarified that in the case that average time interval of LDC is adopted as a time unit, trajectories of paramecia can be regarded as random walk motions.

Fourth, in the numerical simulations the optimum value for the probability of direction change that maximizes the evaluation function was obtained.

## REFERENCES

- DOUGLASS, J. K., WILKENS, L., PANTAZELOU, E. and MOSS, F. (1993) Noise enhancement of information transfer in crayfish mechanoreceptors by stochastic resonance, *Nature*, **365**, 337–340.
- HARA, H. (1984) Anomalous temperature dependence of diffusion coefficient, *Phys. Rev.*, **31**, 4612–4617.
- LEHMER, D. H. (1951) Mathematical models in large-scale computing units, *Ann. Comput. Lab.* (Harvard University), **26**, 141–146.
- NAITO, Y. (1990) *Behavior of Unicellular Animals*, Tokyo University Press, pp. 46–49 (in Japanese).
- NAKAOKA, Y. and OSAWA, F. (1977) Temperature sensitive behaviors of *Paramecium caudatum*, *J. Protozool.*, **24**, 575–580.
- NAKAOKA, Y. and TOYOTAMA, H. (1980) Thermotaxis of paramecium, *Biophysics*, **20**, 335–340 (in Japanese).
- OOTA, T. (2000) *Physics in Non-equilibratory Systems*, Shokabou Ltd., pp. 87–90 (in Japanese).
- OSAWA, F. (2001) Autonomy, voluntariness and individual difference, in *Biophysics of Complex Systems* (ed. K. Kaneko), pp. 155–192, Kyoritsu Syuppan Ltd. (in Japanese).
- RUSSEL, D. F., WILKENS, L. and MOSS, F. (1999) Use of behavioral stochastic resonance by paddle fish for feeding, *Nature*, **402**, 291–294.
- SATO, T. and FUJIMURA, J. (1992) Reaction of paramecium to temperature gradients and the telegraph equation, *J. Phys. Soc. Japan*, **61**, 385–390.
- SHIKATA, Y., SHIKATA, A., SHIMO, R., TAKADA, H., KATO, C., ITO, M., ODA, T. and MIHASHI, K. (1994) Statistical analysis on the angle fluctuation of the direction of a single F-actin sliding on the surface-fixed H-meromyosin, *Proc. Japan Acad.*, **70**, Ser. B, 117–120.
- SHIMO, R. and MIHASHI, K. (2001) Fluctuation of local points of F-actin sliding on the surface-fixed H-meromyosin molecules in the presence of ATP, *Biophysical Chemistry*, **93**, 23–35.
- SUGINO, K. and NAITO, Y. (1988) Measuring method for the swimming trajectories of *Paramecia*, *Science of Organism*, **39**, 485–490 (in Japanese).
- TAKADA, H., KITAOKA, Y. and SHIMIZU, Y. (2001) Mathematical index and model in stabirometry, *FORMA*, **16**, 17–46.
- TAKAYASU, H. (1986) *Fractal*, Asakura Syuppan Ltd., pp. 137–144 (in Japanese).